Journal of Southeast University (English Edition) Vol. 32, No. 2, pp. 201 - 207 June 2016 ISSN 1003—7985

Experimental analysis of the slip sinkage effect based on real vehicle test

Yang Fan[1,2] Lin Guoyu[1] Zhang Weigong[1] Wang Ningbo[1]

([1]School of Instrument Science and Engineering, Southeast University, Nanjing 210096, China)
([2]The 14th Research Institute, China Electronics Technology Group Corporation, Nanjing 210013, China)

Abstract: To improve the semi-empirical model, the slip sinkage effect is analyzed based on the real vehicle test. A dynamic testing system is used to gain the dynamic responses of wheel-soil interactions. The Gauss-Newton algorithm is adopted to estimate the undetermined parameters involved in the slip sinkage models. Wong's original model is compared with three typical slip sinkage models on the prediction performance of a drawbar pull. The maximum error rate, root mean squared error and correlation coefficient are utilized to evaluate the performance. The results indicate that the slip sinkage models outperform Wong's model and greatly improve the prediction accuracy. Lyasko's model is confirmed as an outstanding one for its comprehensive performance. Hence, the existence of the slip sinkage effect is validated. Lyasko's model is selected as an optimal one for the practical evaluation of military vehicle trafficability.

Key words: vehicle trafficability; slip sinkage effect; Gauss-Newton algorithm; real vehicle test; wheel force transducer
doi: 10.3969/j.issn.1003-7985.2016.02.012

Terramechanics is a specialized science branch, with which vehicle trafficability can be evaluated. It is of great importance for the design, control and evaluation of vehicles and planet exploration rovers. The issue of military vehicle trafficability is emphatically studied in this paper. Good vehicle trafficability guarantees good transport capacity, which is a crucial premise for fulfilling a military mission. However, due to adverse field conditions, military vehicles may suffer from non-geometric hazards, such as mud, bog, clay, sand, and snow, in addition to unknown obstacles. These terrains tend to cause the wheels to sink deeply into the surface. It can lead to energy loss or even mission failure. Hence, it is important and essential to evaluate vehicle trafficability before military missions.

Among the existing evaluation models of vehicle trafficability, the semi-empirical model is a typical one, particularly for heavy vehicles. It was pioneered by Bekker et al.[1-2] and later by Wong et al.[3-4] to predict the tractive performance of vehicles. Two analog devices are utilized in this model to represent the wheel-soil interactions. The vertical deformation of soil under load is assumed to be analogous to the soil deformation under a flat plate, while shear deformation of soil under a traction force is assumed to be equal to the shear caused by a rectangular grouser unit. The assumptions contribute to simplify the model and make the model realizable. Although the model is widely used, there is still a series of limitations of the model, for example, the neglect of the slip sinkage effect[5]. The model needs further modifications for a better estimation of wheel-soil interactions.

The issue of the slip sinkage effect is addressed in this paper, which represents an increase of wheel sinkage due to slip. Slip sinkage has been a subject of study since the early stage of development of terramechanics. Reece[6] mentioned the issue 50 years ago with no ideal solution. Bekker[2] pointed out that the prediction of wheel sinkage with the analytical equation deduced from his pressure-sinkage model would not be accurate if there was significant slip sinkage. Azimi et al.[7] observed again that the slip sinkage effect was not included in either the Bekker model or the Wong-Reece model. Ding et al.[8] proposed that dynamic sinkages such as slip sinkage, skid sinkage, and steering sinkage were not reflected in conventional pressure-sinkage models. In recent years, significant progress has been made to solve the problem. Ding et al.[9] investigated the slip sinkage problem of the lunar rover with a single-wheel testbed. A mathematical model for calculating slip sinkage was developed according to vertical load and slip ratio. Lyasko[10] presented an analytical and quantitative evaluation of slip sinkage. The author compared Reece's model[6] with Vasil'ev's model[11] and then proposed an effective analytical formula. Knuth et al.[12] used the discrete element method (DEM) to simulate the slip sinkage phenomena. However, Wong[13] pointed out that a generally accepted method was lacking for predicting slip sinkage in relation to terrain characteristics, design parameters, and operation conditions of the wheel, including wheel slip.

The applicability of the slip sinkage models for military

Received 2015-09-15.
Biographies: Yang Fan (1988—), male, graduate; Lin Guoyu (corresponding author), male, doctor, professor, andrew.lin@seu.edu.cn.
Foundation items: The National Natural Science Foundation of China (No. 51305078), the Science and Technology Plan of Suzhou City (No. SYG201303).
Citation: Yang Fan, Lin Guoyu, Zhang Weigong, et al. Experimental analysis of the slip sinkage effect based on real vehicle test[J]. Journal of Southeast University (English Edition), 2016, 32(2): 201 - 207. doi: 10.3969/j.issn.1003-7985.2016.02.012.

usage needs to be verified. Ding's model is intended for small lunar rovers with diameters smaller than 500 mm while Lyasko's model does not explore applicability. Moreover, the models are mainly validated through indoor testbeds rather than real vehicle tests. Real vehicle conditions demonstrate distinct characteristics, particularly the dynamic responses. For practical applications, real vehicle tests are essential.

In this study, an experimental analysis is conducted on the slip sinkage effect based on the real vehicle test data. A dynamic testing system is presented to gather the dynamic responses of wheel-soil interactions. The Gauss-Newton (GN) algorithm is adopted to determine the parameters involved in the models. The validated model is of great significance in the evaluation of military vehicle trafficability.

1 Methodology

1.1 Slip sinkage model

Wong's straight line model is introduced as an example of the semi-empirical models to lay a theoretical foundation for the experimental validation of the slip sinkage models[4].

As shown in Fig. 1, when a driving torque T and a vertical load W are applied to the wheel, shear force τ develops at the wheel-soil interface and a normal stress distribution σ is created to balance the vertical load.

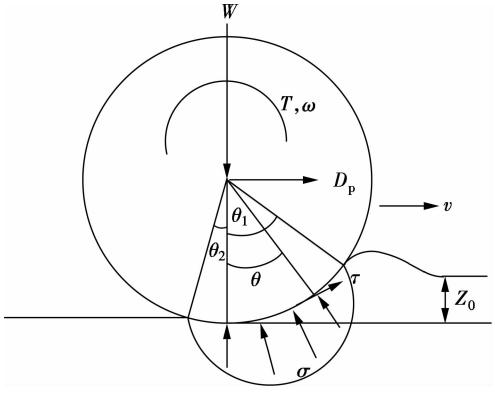

Fig. 1 Wong's semi-empirical model

The angle from the vertical to where the wheel first makes contact with the terrain is denoted by θ_1, called the entrance angle. The angle from the vertical to where the wheel finally loses contact with the terrain is denoted by θ_2, called the exit angle. In real life situations, since θ_2 is usually small and negligible for low cohesion soils, θ_2 is usually assumed to be zero. Z_0 means the total wheel sinkage, which can be used to calculate the entrance angle θ_1:

$$\theta_1 = \arccos\left(1 - \frac{Z_0}{r}\right) \tag{1}$$

where r is the wheel radius.

On the basis of Bekker's pressure-sinkage model[2], the normal stress distribution σ is given as

$$\sigma = \left(\frac{k_c}{b + k_\varphi}\right) Z^n \tag{2}$$

$$Z(\theta) = r(\cos\theta_1 - \cos\theta) \tag{3}$$

where $Z(\theta)$ is the wheel sinkage at θ; k_c is the cohesion module; k_φ is the friction module of soil; n is the sinkage exponent; b is the width of the wheel-soil contact patch. It can be seen that k_c, k_φ, and n are the pressure-sinkage coefficients of the terrain, which characterize normal pressure from a vehicle with sinkage in the terrain.

The expression for the shear stress distribution τ under a wheel formulated by Janosi et al.[14] is adopted as

$$\tau(\theta) = (c + \sigma(\theta)\tan\varphi)[1 - e^{-j(\theta)/K}] \tag{4}$$

$$j(\theta) = r[\theta_1 - \theta - (1 - s)(\sin\theta_1 - \sin\theta)] \tag{5}$$

where the parameter j is the shear displacement and it is a function of θ; c is the cohesion of soil; φ is the internal friction angle of soil; K is the shear deformation modulus; and s is the slip ratio. c, φ, and K characterize the shearing capacity of the terrain. The slip ratio s also plays an important role in defining the shear force. It should be pointed out that only the longitudinal slip is considered in the model. The wheel slip ratio can be calculated by

$$s = \frac{r\omega - V}{r\omega} \tag{6}$$

where V is the linear velocity of the vehicle, and ω is the angular velocity of the wheel.

In this way, the vertical load W, drawbar pull D_p and driving torque T can be predicted as

$$W = rb\left(\int_0^{\theta_1}\sigma(\theta)\cos\theta\mathrm{d}\theta + \int_0^{\theta_1}\tau(\theta)\sin\theta\mathrm{d}\theta\right) \tag{7}$$

$$D_p = rb\left(\int_0^{\theta_1}\tau(\theta)\cos\theta\mathrm{d}\theta - \int_0^{\theta_1}\sigma(\theta)\sin\theta\mathrm{d}\theta\right) \tag{8}$$

$$T = r^2 b\int_0^{\theta_1}\tau(\theta)\,\mathrm{d}\theta \tag{9}$$

The total wheel sinkage can be expressed as[4]

$$Z_0 = \left[\frac{3W}{\sqrt{2r}(k_c + bk_\varphi)(3 - n)}\right]^{2/(2n+1)} \tag{10}$$

It can be inferred that the slip sinkage phenomenon is not included in Wong's model according to Eq. (10). Z_0 is merely a reflection of the static sinkage. To accurately predict the drawbar pull of a vehicle in a given soil, the slip sinkage effect as a dynamic response should be taken into account. Several effective solutions in different forms are listed as follows and their performance on heavy vehicles is to be verified.

Vasil'ev et al.[11] found an analytical formula for calculating vehicle sinkage Z, which was initially proposed for tracked vehicles.

$$Z = Z_0 + Hs \tag{11}$$

where H is the model parameter, and its value can only be obtained experimentally.

An effective analytical formula was developed by Lyasko[10]. The author pointed out that the formula was particularly suitable for motion resistance prediction of tracked and wheeled vehicles, and it was verified by many tests with different wheeled, tracked, and rubber belted vehicles under various soil conditions. A formula with two undetermined coefficients, m_1 and m_2, is expressed as

$$Z = \frac{1 + m_1 s}{1 - m_2 s} Z_0 \tag{12}$$

To estimate slip sinkage, Ding et al.[9] proposed a model using a variant sinkage exponent N as a function of slip ratio to replace the constant sinkage exponent n, and n_1 is the model parameter.

$$N = n + n_1 s \tag{13}$$

1.2 Gauss-Newton algorithm

As a typical nonlinear parameter estimation approach, the Gauss-Newton (GN) algorithm has shown its effectiveness in parameter estimation problems with high accuracy, rapid convergence and high efficiency[15-16]. Considering its outstanding capacity, the GN algorithm is adopted to estimate the undetermined coefficients involved in the slip sinkage models. The detailed description of the GN algorithm can be found in Ref. [16]. The concrete implementation process is illustrated in Fig. 2. The measured physical quantities, such as vehicular dynamic parameters, W, D_p, T, and s, and terrain parameters, c, φ, K, k_c, k_φ, and n, are set to be the inputs $x(k)$ with the combination of the slip sinkage models. The coefficients, H, m_1, m_2, and n_1, in the slip sinkage models make the outputs $\Theta(k)$. It works by iteratively modifying an initial estimate of undetermined coefficients and reaches a converged solution after a number of iterations. $\boldsymbol{J}_k$ is defined as the sensitivity matrix of the GN method while k means the iteration number. The iterative process stops when the error between the indentified value and the current value falls below a predefined threshold ε.

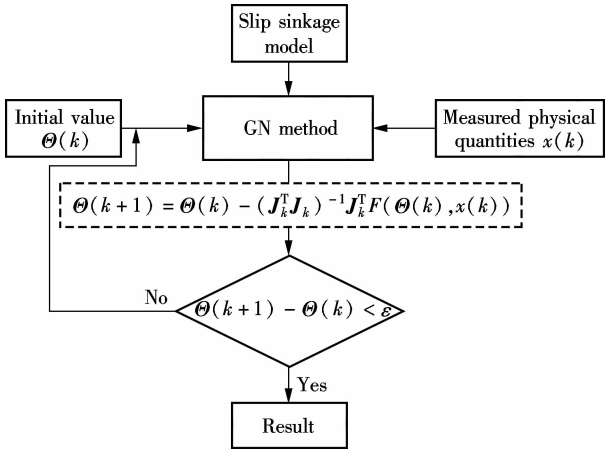

Fig. 2 Flow diagram of the GN model

1.3 Satisfactory criteria

To evaluate the performance of the slip sinkage models, several common numerical criteria, such as the maximum error rate M_0, root mean squared error R_0, and the correlation coefficient R^2, are imported in this study. R_0 and R^2 are given as

$$R_0 = \left[\frac{1}{N}\sum_{i=1}^{N}(y_{p,i} - y_{a,i})^2\right]^{1/2}$$

$$R^2 = \left[\frac{\mathrm{cov}(y_a, y_p)}{\sigma_{y_a}\sigma_{y_p}}\right]^2$$

$$\mathrm{cov}(y_a, y_p) = \frac{1}{N}\sum_{i=1}^{N}(y_{a,i} - \bar{y}_a)(y_{p,i} - \bar{y}_p)$$

where $\mathrm{cov}(y_a, y_p)$ is the covariance between the actual and the predicted values; y_a is the actual value while y_p refers to the predicted value; $\bar{y}_a$ and $\bar{y}_p$ denote the average result of the actual and predicted values, respectively; and σ_y is the relevant standard deviation. The smaller value of R_0 indicates a higher accuracy of the predicted value and a higher correlation value expresses a good prediction performance.

2 Experimental Data Acquisition

2.1 Dynamic testing system

A dynamic testing system is presented to obtain real vehicle test data[17]. It consists of several primary sensors, such as the wheel force transducer (WFT), wheel speed sensor, and GPS, as shown in Fig. 3(a). The WFT adopted in the system is developed by Southeast University[18] and can be fixed on real vehicles to measure the vertical load, drawbar pull, and driving torque. The GPS gathers the linear velocity V and the wheel speed sensor to measure the angular speed ω. Then, the slip ratio can be calculated by Eq. (6). The signals from various sensors are gathered by an integrated data acquisition system synchronously and real-timely, as shown in Fig. 3(b). Thus, an instrumented vehicle equipped with the dynamic testing system makes it possible to conduct field tests for experimental validation.

2.2 Test procedure

Field tests were conducted in order to obtain the essential data for experimental validation. For this purpose, a wide range of slip ratio and wheel sinkage should be guaranteed. So amongst all the driving maneuvers, the straight accelerate-brake driving was adopted. It can provide the most desirable range of data. As a 3.6-t military vehicle is used in the test, the static vertical load on the left rear wheel is about 8 kN. The data presented in this study is based on the field tests conducted on a Dingyuan

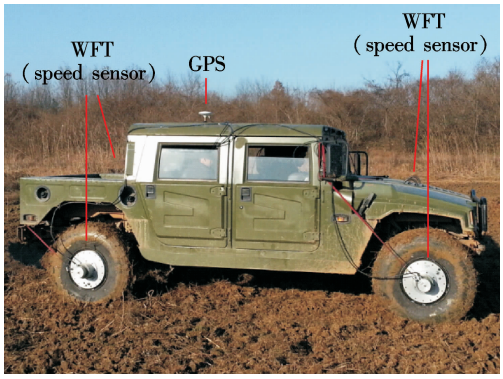

(a)

(b)

Fig. 3 Dynamic testing system. (a) Test vehicle equipped with WFT and GPS; (b) Integrated data acquisition system

proving ground in An'hui province, China on December 11, 2014. Various terrains were selected for field tests, such as sandy soil, clay soil, and sandy loam. The presented test data in this study are mainly from the clay soil and sandy soil. The test procedures are described as follows: 1) The soil was collected and transported back to the soil test laboratory for the specific analysis of terrain parameters. The experimental procedure of measuring the terrain parameters is similar to that found in Ref. [19]. 2) It took several minutes to confirm the GPS signal. Then all the other devices were turned on and checked that they were working under normal conditions. 3) The vehicle equipped with the testing system was tested along with the planned route and the dynamic responses were recorded by the data acquisition system. 4) The test on each kind of terrain was conducted for over five times to guarantee its reliability.

3 Experimental Validation of Slip Sinkage Models

Based on the abundant real vehicle test data, experimental validation can be done. It aims to select a preferable slip sinkage model for military vehicles. The relevant terrain parameters are shown in Tab. 1. As we can see from the introduction of the dynamic testing system, no wheel sinkage is directly measured. The accuracy of the vision-based sinkage estimation model remains to be improved[20]. So, in this paper, the slip sinkage effect is investigated through its effect on the prediction performance of a drawbar pull. The drawbar pull is a critical evaluation index of vehicle trafficability. Based on the data curves of the drawbar pull vs. time, a Matlab GUI program was developed to draw the curves of the drawbar pull vs. slip ratio.

Tab. 1 Relevant terrain parameters of clayed soil and sandy soil

Soil type	Shear strength parameters				Pressure sinkage parameters	
	c/kPa	φ/(°)	K/m	n	k_c/(kN · m$^{-(n+1)}$)	k_φ/(kN · m$^{-(n+2)}$)
Clay soil	7.58	14	0.025	0.85	43.68	499.3
Sandy soil	1.00	25	0.025	1.04	1.00	580.0

A representative example of the field test data on clay soil is shown in Fig. 4. The presented data is provided by a test travel with an additional vertical load of 3 kN and an inflation pressure of 340 kPa. Owing to the straight accelerate-brake driving maneuver, a wide range of slip ratio is obtained. After appropriate filtering, the fine continuity of the curves is demonstrated as a whole.

Fig. 4(a) shows the comparison result of the test data with the simulation result of Wong's semi-empirical model. A distinct difference between the two curves is indicated by M_0 of 254.5% and R_0 of 208.7 N, as shown in Tab. 2. The correlation analysis is also done with the result of 0.909 7. It indicates that the drawbar pull is not well predicted by Wong's original model. As mentioned above, the slip sinkage effect may be a primary cause of the distinct errors. It is to be verified in the following analysis.

Three typical slip sinkage models, such as Vasil'ev's model, Lyasko's model, and Ding's model, are adopted for a validation study. The corresponding formulas are expressed as Eq. (11) to (13). The forms of the formulas are imposed and the related coefficients are determined in accordance with the real test situations. The GN algorithm is utilized to calculate the coefficients with the results shown in Tab. 3. In turn, the confirmed formulas are used to predict the drawbar pull, as shown in Figs. 4 (b) to (d). The numerical analysis of the curves is listed in Tab. 2. It is worth pointing out that the curve segment with the slip ratio of smaller than 0.2 is not included in the numerical analysis. Small values of the drawbar pull can easily be influenced by the measurement uncertainty in the tests. Also, it has a negative effect on the analysis of the integral prediction performance. In general, the slip sinkage models indeed help to improve the prediction accuracy of the drawbar pull. It is good evidence for the existence of the slip sinkage effect, and it has significant

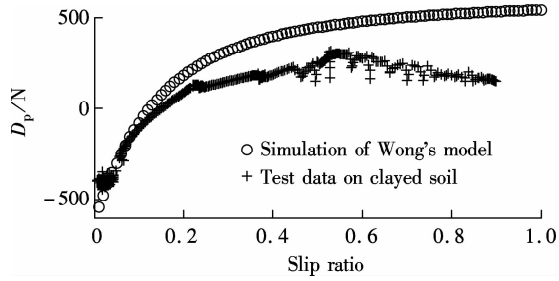

(a)

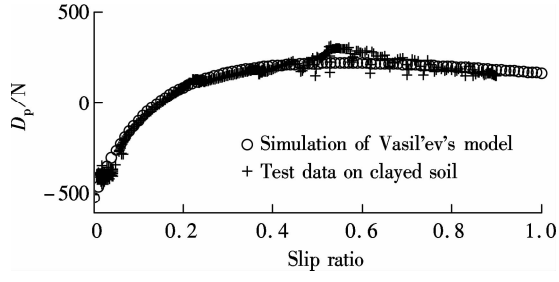

(b)

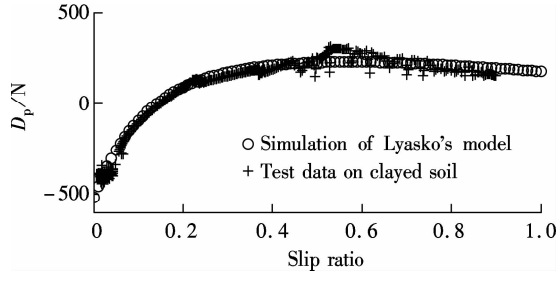

(c)

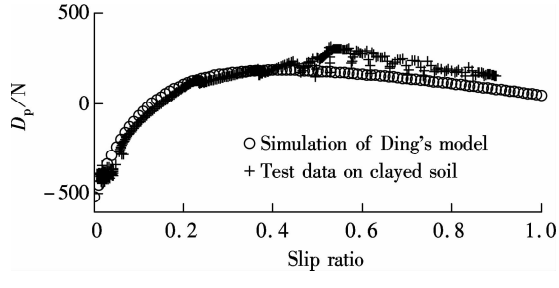

(d)

Fig. 4 Comparisons of test data on clay soil with simulation results of different models. (a) Simulation of Wong's model; (b) Simulation of Vasil'ev's model; (c) Simulation of Lyasko's model; (d) Simulation of Ding's model

impact on the semi-empirical model. On the other hand, remarkable differences are shown among the three slip sinkage models. Vasil'ev's model and Lyasko's model have better performance than that of Ding's model on clay soil. Vasil'ev's model obtains the smallest M_0 of 38.02% while Lyasko's model performs the smallest R_0 of 32.24 N. The correlation analysis result further demonstrates their good performance, 0.988 1 for Vasil'ev's model and 0.988 3 for Lyasko's model. However, generally speaking, Ding's model still outperforms Wong's original model.

Tab. 2 Numerical analysis results of four prediction models on clay soil with $s > 0.2$

Model	M_0/%	R_0/N	R^2
Wong's model	254.50	208.70	0.909 7
Vasil'ev's model	38.02	32.62	0.988 1
Lyasko's model	40.78	32.24	0.988 3
Ding's model	59.71	67.53	0.964 3

Tab. 3 Estimation results of the slip sinkage coefficients

Model	Vasil'ev's model	Lyasko's model		Ding's model
	H	m_1	m_2	n_1
Clayed soil	0.02	0.1	0.05	0.35
Sandy soil	0.08	0.6	0.03	0.53

For a further validation of the slip sinkage effect on various terrains, the field test data on sandy soil are presented in Fig. 5. The data used is from the test travel with

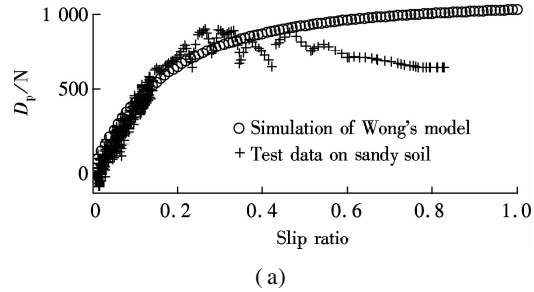

(a)

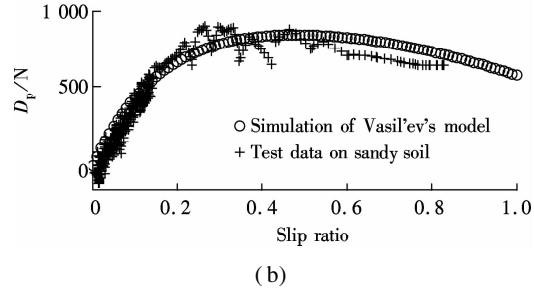

(b)

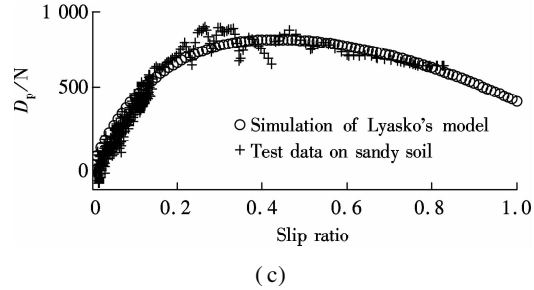

(c)

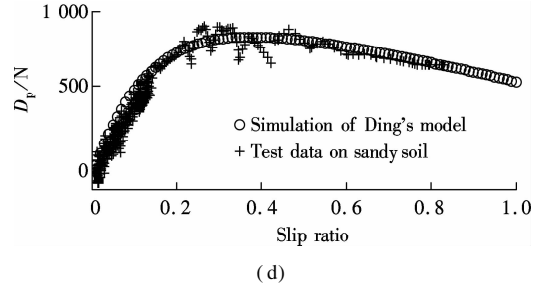

(d)

Fig. 5 Comparisons of test data on sandy soil with simulation results of different methods. (a) Simulation of Wong's model; (b) Simulation of Vasil'ev's model; (c) Simulation of Lyasko's model; (d) Simulation of Ding's model

an additional vertical load of 5 kN and an inflation pressure of 340 kPa. A similar analysis progress is demonstrated as follows. Fig. 5(a) shows the comparison of the simulation result of Wong's model with the field test data. Remarkable prediction errors are also highlighted with M_0 of 98.45%, R_0 of 183.00 N, and R^2 of 0.910 4, as shown in Tab. 4. According to the estimation results of the slip sinkage coefficients in Tab. 3, the prediction results of the three slip sinkage models are shown in Figs. 5 (b) to (d). The detailed numerical analysis is listed in Tab. 4. Similarly, to avoid the adverse influence of measurement uncertainty in field tests, the range of slip ratio is set to be from 0.1 to 1.0. The three slip sinkage models outperform Wong's model. The same conclusion can be obtained that the slip sinkage effect is a non-negligible issue and should be taken into consideration in the semi-empirical model. By contrast, Lyasko's model and Ding's model outperform Vasil'ev's model on sandy soil. Lyasko's model obtains the smallest M_0 of 25.85% while Ding's model performs the smallest R_0 of 58.51 N. The corresponding correlation analysis result is also a good representation of this point.

Tab. 4 Numerical analysis results of four prediction models on sandy soil with $s > 0.1$

Model	M_0/%	R_0/N	R^2
Wong's model	98.45	183.00	0.910 4
Vasil'ev's model	39.33	89.37	0.965 6
Lyasko's model	25.85	69.14	0.979 0
Ding's model	26.95	58.51	0.974 4

4 Conclusion

The issue of the slip sinkage effect involved in the semi-empirical model is addressed in this paper. An experimental analysis is done based on real vehicle test data. A comparison is made between Wong's original model and three typical slip sinkage models. Simulation results show that the slip sinkage models outperform Wong's model whether on clay soil or on sandy soil. It can be inferred that the slip sinkage effect is an integral part of the semi-empirical model. For practical usage, the slip sinkage effect should be taken into consideration. Moreover, Lyasko's model demonstrates the most comprehensive performance. So it is selected as a preferable model for the practical evaluation of military vehicle trafficability.

References

[1] Bekker M G. *Theory of land locomotion*: *The mechanics of vehicle mobility* [M]. Ann Arbor, USA: The University of Michigan Press, 1956.

[2] Bekker M G. *Introduction to terrain-vehicle system* [M]. Ann Arbor, USA: The University of Michigan Press, 1969.

[3] Wong J Y. *Terramechanics and off-road vehicle* [M]. Amsterdam, Holland: Elsevier, 1989.

[4] Wong J Y. *Theory of ground vehicles* [M]. New York: John Wiley & Sons, 2008.

[5] Tiwari V K, Pandey K P, Pranav P K. A review on traction prediction equations [J]. *Journal of Terramechanics*, 2010, **47**(3): 191 − 199. DOI: 10.1016/j.jterra.2009.10.002.

[6] Reece A R. Principles of soil-vehicle mechanics [J]. *Proceedings of the Institution of Mechanical Engineers*: *Automobile Division*, 1965, **180**(1): 45 − 66.

[7] Azimi A, Kovecses J, Angeles J. Wheel-soil interaction model for rover simulation and analysis using elastoplasticity theory [J]. *IEEE Transactions on Robotics*, 2013, **29**(5): 1271 − 1288. DOI: 10.1109/tro.2013.2267972.

[8] Ding L, Gao H B, Deng Z Q, et al. New perspective on characterizing pressure-sinkage relationship of terrains for estimating interaction mechanics [J]. *Journal of Terramechanics*, 2014, **52**(1): 57 − 76. DOI: 10.1016/j.jterra.2014.03.001.

[9] Ding L, Gao H B, Deng Z Q, et al. Wheel slip sinkage and its prediction model of lunar rover [J]. *Journal of Central South University of Technology*, 2010, **17**(1): 129 − 135. DOI: 10.1007/s11771-010-0021-7.

[10] Lyasko M. Slip sinkage effect in soil-vehicle mechanics [J]. *Journal of Terramechanics*, 2010, **47**(1): 21 − 31. DOI: 10.1016/j.jterra.2009.08.005.

[11] Vasil'ev A V, Dokychaeva E N, Utkin-Lubovtsov O L. Effect of tracked tractor design parameters on tractive performance [R]. Moscow: Mashinostroenie, 1969.

[12] Knuth M A, Johnson J B, Hopkins M A, et al. Discrete element modeling of a Mars Exploration Rover wheel in granular material [J]. *Journal of Terramechanics*, 2012, **49**(1): 27 − 36. DOI: 10.1016/j.jterra.2011.09.003.

[13] Wong J Y. Predicting the performances of rigid rover wheels on extraterrestrial surfaces based on test results obtained on earth [J]. *Journal of Terramechanics*, 2012, **49**(1): 49 − 61. DOI: 10.1016/j.jterra.2011.11.002.

[14] Janoshi Z, Hanamoto B. An analytical determination of drawbar pull as a function of slip for tracked vehicles in deformable soils [C]//*The 1st International Conference on the Mechanics of Moil-Vehicle Systems*. Turin, Italy, 1961: 132 − 138.

[15] Tao T, Nehorai A. Information-driven distributed maximum likelihood estimation based on Gauss-Newton method in wireless sensor networks [J]. *IEEE Transaction Signal Processing*, 2007, **55**(9): 4669 − 4682.

[16] Yao L H, Guo Y F. Hybrid algorithm for parameter estimation of the groundwater flow model with an improved genetic algorithm and Gauss-Newton method [J]. *Journal of Hydrologic Engineering*, 2014, **19**(3): 482 − 494. DOI: 10.1061/(asce)he.1943-5584.0000823.

[17] Yang F, Lin G Y, Zhang W G. A new dynamic testing system for wheel-soil interactions [C]//*IEEE Instrumentation and Measurement Technology Conference*. Pisa, Italy, 2015: 1331 − 1336.

[18] Lin G Y, Zhang W G, Yang F, et al. An initial value calibration method for the wheel force transducer based on memetic optimization framework [J]. *Mathematical Problem in Engineering Paper*, 2013, **2013**: 275060-1 − 275060-10. DOI: 10.1155/2013/275060.

[19] Smith W, Melanz D, Senatore C, et al. Comparison of

DEM and traditional modeling methods for simulating steady-state wheel-terrain interaction for small vehicles [C]//*Proceedings of the 7th Americas Regional Conference of the ISTVS*. Tampa, FL, USA, 2013: 1 - 16.

[20] Reina G, Ojeda L, Milella A, et al. Wheel slippage and sinkage detection for planetary rovers [J]. *IEEE/ASME Transactions on Mechatronics*, 2006, **11**(2): 185 - 195. DOI: 10.1109/tmech.2006.871095.

基于实车试验的滑转沉陷效应实验分析

杨 帆[1,2] 林国余[1] 张为公[1] 王宁波[1]

([1] 东南大学仪器科学与工程学院, 南京 210096)
([2] 中国电子科技集团公司第十四研究所, 南京 210013)

摘要:为了改进半经验模型,基于实车试验对滑转沉陷效应进行了分析. 通过实车动态测试系统采集轮壤间的相互作用响应,并采用高斯牛顿迭代算法估计滑转沉陷模型参数. 比较了 Wong 的原始模型与 3 种典型滑转沉陷模型在挂钩牵引力上的预测表现. 引入最大误差率、均方根误差和相关系数作为评价指标. 实验结果表明,滑转沉陷模型效果均好于原始模型,极大地提高了挂钩牵引力的预测准确性,尤以 Lyasko 模型综合性能最为突出. 因此,实验结果验证了滑转沉陷效应的存在性. 选定 Lyasko 模型作为最佳模型应用于军用车辆通过性的实际评价工作中.

关键词:车辆通过性;滑转沉陷效应;高斯-牛顿法;实车试验;车轮力传感器
中图分类号:U461.5